EPR Study of VO²⁺ Center in Fast Proton Conductor K₃H(SO₄)₂

A. Ostrowski*, S. Waplak and W. Bednarski

Institute of Molecular Physics, Polish Academy of Sciences
Smoluchowskiego 17, 60-179 Poznań, Poland

The pretransitional phenomena of superprotonic phase transition ($T_{sp} = 471$ K) were studied in detail by X-band continuous wave EPR spectra of $K_3H(SO_4)_2$ crystal doped with VO^{2+} ions. Three kinds of VO^{2+} complexes (magnetically equivalent but structurally non-equivalent) denoted as VO^{2+}(I), VO^{2+}(II), and VO^{2+}(III) were found. "Smearing out" of the superhyperfine structure was observed as a result of interbond proton motion. VO^{2+} impurity replaces K^+ ion and experiences the same average crystal field gradient at $T_{sp} = 471$ K for I- and II-type complexes. The increase in interbond proton frequency hopping above 360 K is a reason of significant line broadening.

PACS numbers: 61.50.–f, 76.30.–v

1. Introduction

Crystals, which belong to family $M_3H(XO_4)_2$, where M = NH$_4$, Rb, Cs, K; X = S, Se, exhibit a high proton conductivity [1–7]. The crystal structure of $K_3H(SO_4)_2$ (KHS) was determined by X-ray diffraction [8, 9]. The thermal anomaly at about 478 K was found in differential scanning calorimetry (DSC) measurements and attributed to the superprotonic phase transition [6]. Below this temperature KHS belongs to the space group $A2/a$ [8, 9] and exhibits ferroelastic properties [6]. Until now the structure of KHS in the superprotonic phase is unknown [7].

The aim of this work is EPR study of the lattice dynamic of $K_3H(SO_4)_2$ crystal doped with VO^{2+} below the temperature of superprotonic phase transition ($T_{sp} = 471$ K). In the previous paper we presented the EPR study of KHS crystal

---

*corresponding author; e-mail: ostrowski@ifmpan.poznan.pl

doped with Cu^{2+} ions [10]. It was found that the pretransitional phenomena were manifested in the spin-Hamiltonian (SH) parameters and the line width ΔH_{pp} depends on temperature. We supposed that doping with the other paramagnetic impurity having different nuclear spin value and coordination in the crystal lattice, would enable better understanding of charge transfer properties in KHS.

2. Experimental

Hexagonal plate-like $K_3H(SO_4)_2$ crystals were grown isothermally at 300 K from the saturated aqueous solution containing 19 wt% K_2SO_4, 12.7 wt% H_2SO_4, and 0.3 wt% $VOSO_4 \cdot 4H_2O$. Optical investigation of the single crystal in polarized light reveals the ferroelastic $n \cdot 60°$ domain pattern. EPR studies were carried out on a single-domain sample cut out under the polarization microscope. The XYZ orthogonal laboratory frame chosen for the EPR anisotropy measurement was related to the a, b, and c crystallographic axes as follows: $X \parallel a$, $Y \parallel b$, and $Z \parallel a \times b$. The EPR study was performed with a RADIOPAN X-band continuous wave (CW) spectrometer and a BRUKER EMX Q-band spectrometer.

3. Spin-Hamiltonian parameters and coordination of VO^{2+} ions in KHS

Figure 1 shows the EPR spectrum with an external magnetic field $\boldsymbol{B}$ parallel to the Y-axis. Three types of VO^{2+} complexes (the same SH parameters but different coordination planes) denoted as $VO^{2+}(I)$, $VO^{2+}(II)$, and $VO^{2+}(III)$ were found at room temperature (RT). The spectral intensity of the signal ascribed to $VO^{2+}(III)$ complex was about ten times smaller than that for $VO^{2+}(I)$ and $VO^{2+}(II)$ complexes.
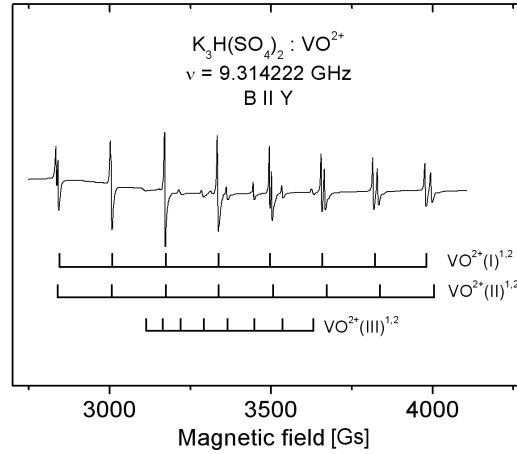
Fig. 1. The EPR spectra of the single-domain $K_3H(SO_4)_2$:VO^{2+} crystal at room temperature. The external magnetic field B is parallel to the Y-axis.

Figure 2 presents the angular dependence of EPR line for I- and II-type complexes in YZ plane. Due to the point symmetry $2/m$ there are two magnetically equivalent centres for each type of the complexes in the single-domain crystal (see Table).
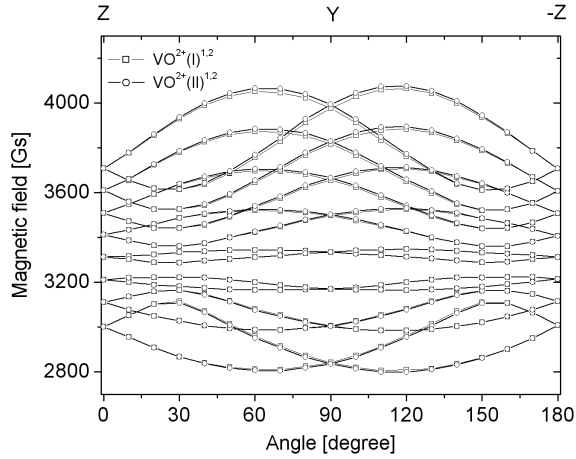
Fig. 2. The angular dependence of resonance fields for VO^{2+}(I) and VO^{2+}(II) complexes in the YZ plane. The symbols represent the experimental data for VO^{2+}(I) (squares) and VO^{2+}(II) (circles) complexes.

TABLE

Spin-Hamiltonian parameters and direction cosines of the VO^{2+}(I)[1,2] and VO^{2+}(II)[1,2] complexes in K$_3$H(SO$_4$)$_2$:VO^{2+} at room temperature.

Complex	Principal g-values	Principal A-values in [Gs]	Direction cosines of the principal of the direction g and A		
			X	Y	Z
VO^{2+}(I)	1.973(3)	73.3(5)	0.596	±0.047	0.802
	1.972(3)	75.7(5)	±0.638	-0.634	∓0.437
	1.918(3)	202.5(5)	0.487	±0.772	0.408
VO^{2+}(II)	1.973(3)	73.3(5)	0.571	±0.084	0.817
	1.972(3)	75.7(5)	±0.681	-0.604	∓0.414
	1.918(3)	202.5(5)	0.458	±0.792	-0.402

The EPR spectrum of VO^{2+} centre is described by the spin Hamiltonian

$$H = \beta \boldsymbol{B}\boldsymbol{g}\hat{S} + \hat{S}\boldsymbol{A}\hat{I}, \tag{1}$$

where $\boldsymbol{g}$ is the spectroscopic tensor, $\boldsymbol{A}$ is the hyperfine tensor, $\hat{S}$ and $\hat{I}$ are the VO^{2+} electronic and nuclear spin operators, respectively.

From the angular dependence of the line positions and hyperfine splitting in three mutually perpendicular planes XY, ZY, ZX, direction cosines of the main directions were determined for both complexes.

To obtain the principal values of g and A tensors we have measured the positions of hyperfine structure resonance lines along the principal directions x, y, z, and applied modified equations [11] described in our previous papers [10, 12]. Table includes the g and A tensors values and their direction cosines for I- and II-type complexes. There is a slight difference ($2°$) between orientation of principal axis system for $VO^{2+}(I)$ and $VO^{2+}(II)$ complexes.

In order to find the coordination plane of the VO^{2+} ion we applied the same procedure as for Cu^{2+} centre [10]. The analysis of the crystal lattice shows two possible sites of VO^{2+} ions:

a) K^+ ion vacancy,

b) the interstitial position between two vacancies of nearest-neighbouring K^+.

In the both cases the nearest oxygen atoms of neighbouring SO_4 groups form the quadrangles, which coordinate VO^{2+} ion.

The angle between the normal to the assumed coordination plane and the main z-axis direction was calculated for both complexes and for all possible configurations. In each case the angle about $3°$ showed that the choice of the VO^{2+} position was still ambiguous. However, the superhyperfine structure (SHFS) at RT was observed. The analysis of the line position and the line width of transition $(M_s = 1/2,\ m = 7/2) \leftrightarrow (M_s = -1/2,\ m = 7/2)$ demonstrated that VO^{2+} ion interacts with two equivalent protons ($I = 1/2$). Figure 3 presents the experimental and simulated spectra. Finally we found that VO^{2+} ion occupies K^+ ion vacancy. The extra charge is compensated by a proton vacancy, because only at this po-
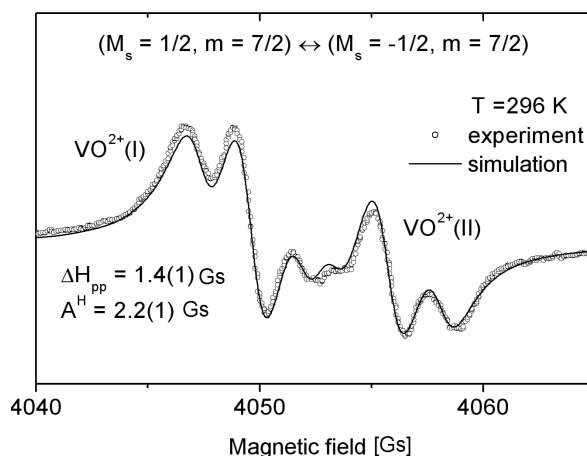
Fig. 3.   The experimental (circles) and simulated (lines) spectrum with superhyperfine structure for VO^{2+} ion in the $K_3H(SO_4)_2$ at RT.
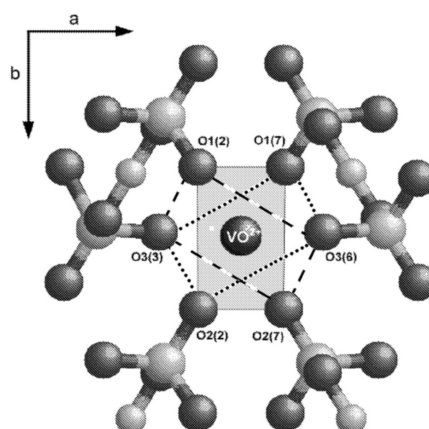
Fig. 4. The position of VO^{2+} ion in the monoclinic phase in KHS crystal. VO^{2+} ion replaces K^+(I) ion. The assumed coordination planes are marked as dotted and dashed quadrangle for I- and II-type and grey quadrangle for III-type complexes, respectively.

sition the interaction of VO^{2+} with two protons of $SO_4^{2-}-H\ldots SO_4^{2-}$ dimers is possible. Figure 4 shows coordination planes as dotted and dashed quadrangle for I- and II-type and grey quadrangle for III-type complexes, respectively. The temperature studies confirmed the above statement, since the intensity of VO^{2+}(III) signal increases above 435 K contrary to I- and II-type lines, for which the spectral intensity decreases. Relative change of intensities unambiguously indicates the same position for all types of complexes with different coordination planes.

A slight difference of principal axis system for VO^{2+}(I) and VO^{2+}(II) complexes is related to VO^{2+} off-centre position and/or different proton vacancy charge compensation. Similar coordination of VO^{2+} ion in $(NH_4)_3H(SO_4)_2$ crystal was determined by Minge and Waplak [13].

4. Temperature dependence of the VO^{2+} spectra below superprotonic phase transition

As has been mentioned above, the SHFS was observed for VO^{2+} centres. Figure 5 shows the temperature evolution of SHFS spectra. A "smearing out" of SHFS with increasing temperature is clearly visible. This behaviour results from the increase in frequency of interbond proton/vacancy motion as the temperature increases. Such effect was previously observed for Cu^{2+} centre [10] in this crystal. This phenomenon appears when proton jump frequency τ_c^{-1} becomes faster than the SHFS splitting A^H (in frequency units) [14]:

$$\tau_c^{-1} \geq A^H/2\pi h. \tag{2}$$

For $A^H = 2.3$ Gs the following value was obtained: $\tau_c^{-1} \approx 3.8 \times 10^7$ Hz. The "smearing out" of SHFS is observed above about 400 K.
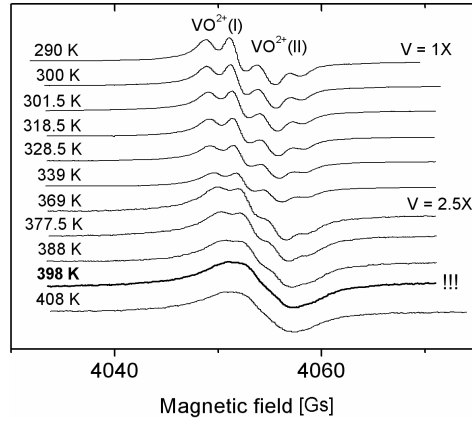
Fig. 5.   Evolution of the superhyperfine (SHF) component of $(M_s = 1/2,\ m = 7/2) \leftrightarrow$ $(M_s = -1/2,\ m = 7/2)$ transition versus temperature for $VO^{2+}(I)$ and $VO^{2+}(II)$ complexes.

Temperature dependence of the resonance lines separation δH of the I- and II-type VO^{2+} complexes is shown in Fig. 6. $VO^{2+}(I)$ and $VO^{2+}(II)$ spectra become identical with increasing temperature. Finally, they have the same direction cosines at temperature $T_{sp} \approx 471$ K.
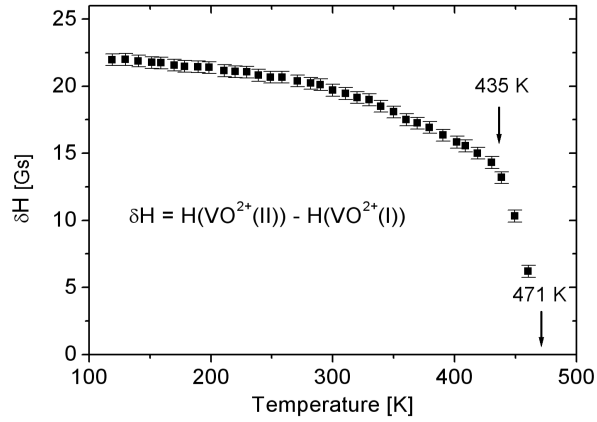
Fig. 6.   The temperature dependence of the separation of resonance lines δH for VO^{2+} complexes in the $K_3H(SO_4)_2$. $\boldsymbol{B} \perp \boldsymbol{Z}$ and $\angle(\boldsymbol{B}, \boldsymbol{Y}) = 5°$.

The temperature dependence of the line width ΔH_{pp} for $VO^{2+}(I)$ and $VO^{2+}(II)$ complexes is shown in Fig. 7. Above 360 K the line is significantly broadened. Additionally, there are minima at 235 K in the $\Delta H_{pp}(T)$ dependences.

Q-band EPR data of the temperature dependences of superhyperfine constant A^H and the line width $\Delta H_{pp}^{(SHFS)}$ are presented in Figs. 8 and 9. Both
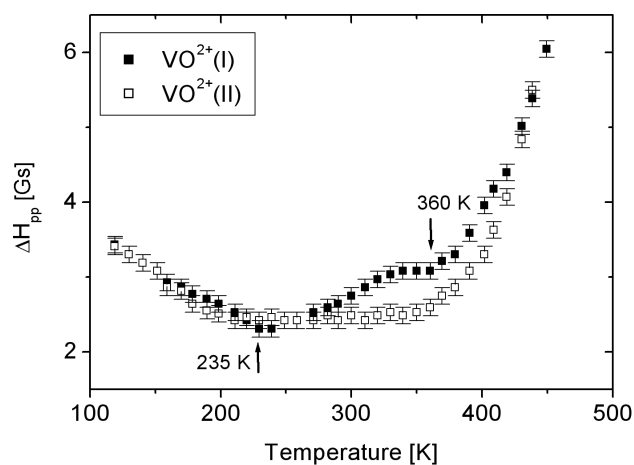
Fig. 7. The line width ΔH_{pp} of the hyperfine component of $(M_s = 1/2,\ m = 7/2) \leftrightarrow (M_s = -1/2,\ m = 7/2)$ transition versus temperature in $K_3H(SO_4)_2{:}VO^{2+}$. $\boldsymbol{B} \perp \boldsymbol{Z}$ and $\angle(\boldsymbol{B}, \boldsymbol{Y}) = 5°$.

parameters were obtained by computer simulations. The superhyperfine constant A^H linearly decreases with increasing temperature. The line width $\Delta H_{pp}^{(SHFS)}$ minima at 108 K and 142 K for $VO^{2+}(I)$ and $VO^{2+}(II)$ were observed.
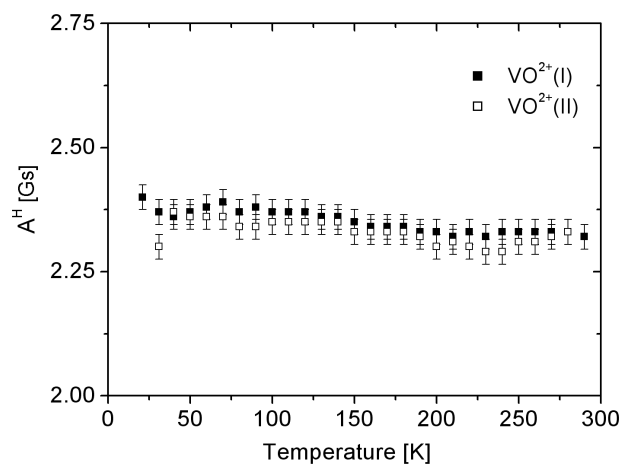
Fig. 8. The temperature dependence of the superhyperfine constant A^H of $VO^{2+}(I)$ and $VO^{2+}(II)$ complexes. Q-band measurement.

Above 435 K we observe gradual changes of spectral intensities: the intensity decreases for I- and II-type and increases for III-type complexes. This behaviour indicates that the position for III-type complex becomes more energetically preferable.
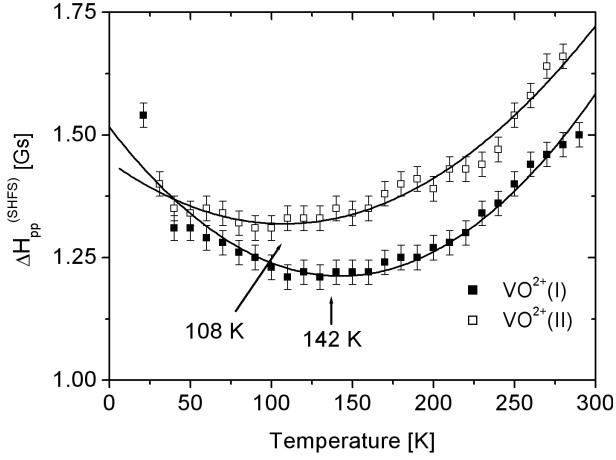
Fig. 9. The temperature dependence of the line width $\Delta H_{pp}^{(SHFS)}$ of SHFS components of VO^{2+}(I) and VO^{2+}(II) complexes. Q-band measurement.

5. Discussion and conclusions

The averaging of VO^{2+}(I) and VO^{2+}(II) direction cosines indicates that VO^{2+} ions experience the same crystal field gradient at 471 K. This process starts rapidly already above 435 K as for III-type complex spectral intensity increases. The averaging of direction cosines is in agreement with Rb^{87} NMR data in isomorphous $Rb_3H(SO_4)_2$ crystal [15], where only one Rb^+ ion position about 50 K below T_{sp} was observed, whereas three positions at RT. This is a result of the averaging of electric field gradient (EFG) tensor experienced by Rb^+/K^+ ions.

Significant increase in ΔH_{pp} line width above 360 K corresponds to the presence of temperature anomaly of crystal field parameter D previously observed in KHS doped with Mn^{2+} [16]. Mn^{2+} and VO^{2+} ions occupy the same position in the crystal lattice. The extra charge is compensated by the proton vacancy. Because D and ΔH_{pp} parameters are sensitive to any change of electric crystal field gradient, the increase in frequency of proton/vacancy motion is reflected as anomalies observed.

The ΔH_{pp} line width differences versus temperature (Fig. 7) for I- and II-type complexes result from the anisotropy of A^H tensor as well as from the anisotropy of spin–lattice relaxation time ($\Delta H_{pp} \propto 1/T_1$). The anisotropy of spin–lattice relaxation rate has already been reported for γ-irradiated $Gly{\cdot}H_3PO_3$ crystal and its deuterated equivalent [16]. This effect was ascribed to hydrogen anisotropy bond dynamics. We recorded minima of the line widths similar as for KHS:Mn^{2+} [17]. These minima may be attributed to two temperature dependent processes of proton/vacancy motion: intrabond and interbond.

The X-ray data of electron density of hydrogen bond performed by Noda et al. reveals that the double well potential of hydrogen bond changes into the single

one below 100 K [9]. The $\Delta H_{\text{pp}}^{\text{(SHFS)}}$ broadening at low temperatures is due to the freezing of protons in slightly different single potential wells (most probably unequal distribution of VO^{2+} impurities in the crystal lattice).

Acknowledgments

References

[1] A.I. Baranov, *Kristallografija* **48**, 1081 (2003).

[2] A.I. Baranov, N.P. Makarova, I.P. Muradjan, A.W. Tregubczenko, L.A. Shuvalov, W.I. Simonov, *Kristallografija* **32**, 682 (1987).

[3] L. Schwalovsky, V. Vinnichenko, A. Baranov, U. Bismayer, B. Merinov, G. Eckold, *J. Phys., Condens. Matter* **10**, 3019 (1998).

[4] A.I. Baranov, V.V. Dolbinina, E.D. Yakushkin, V.Y. Vinnichenko, V.H. Schmidt, S. Lanceros-Mendez, *Ferroelectrics* **217**, 285 (1998).

[5] A. Pawłowski, Cz. Pawlaczyk, B. Hilczer, *Solid State Ionic* **44**, 17 (1990).

[6] Y. Matsuo, J. Hatori, Y. Nakashima, S. Ikehata, *Solid State Commun.* **130**, 269 (2004).

[7] C.R.I. Chisholm, S.M. Haile, *Solid State Ionic* **145**, 179 (2001).

[8] Y. Noda, S. Uchiyama, K. Kafuku, H. Kasatani, H. Terauchi, *J. Phys. Soc. Jpn.* **59**, 2804 (1990).

[9] Y. Noda, S. Uchiyama, Y. Watanabe, H. Terauchi, *J. Phys. Soc. Jpn.* **61**, 905 (1992).

[10] A. Ostrowski, W. Bednarski, S. Waplak, *Acta Phys. Pol. A* **104**, 549 (2003).

[11] U. Sakaguchi, Y. Arata, S. Fujiwara, *J. Magn. Res.* **9**, 118 (1973).

[12] J. Minge, S. Waplak, L. Szczepańska, *Acta Phys. Pol. A* **64**, 151 (1983).

[13] J. Minge, S. Waplak, *Phys. Status Solidi B* **123**, 27 (1984).

[14] C. Evora, V. Jaccarino, *Phys. Rev. Lett.* **39**, 1554 (1977).

[15] J. Dolinšek, U. Mikac, J.E. Javoršek, G. Lahajnar, R. Blinc, *Phys. Rev. B* **58**, 8445 (1998).

[16] J. Goslar, S.K. Hoffman, W. Hilczer, *Solid State Commun.* **121**, 423 (2002).

[17] S. Waplak, *Acta Phys. Pol. A* **86**, 939 (1994).